Hybridized high concentration photovoltaic unit with enhanced performance air gap membrane distillation unit via depositing reduced graphene oxide layer upon the condensation plate using electrophoretic deposition technique

Rabie, Mohammed
Chemical and Petrochemicals Engineering Department, Egypt-Japan University of Science and Technology

M.F. Elkady
Chemical and Petrochemicals Engineering Department, Egypt-Japan University of Science and Technology

Yoshitake, Tsuyoshi
Department of Advanced Energy Science and Engineering, Kyushu University

A.H. El-Shazly
Chemical and Petrochemicals Engineering Department, Egypt-Japan University of Science and Technology

https://hdl.handle.net/2324/7183359

出版情報：Energy Reports. 9, pp.230-238, 2023-03. Elsevier
バージョン：

Available online at www.sciencedirect.com
ScienceDirect
Energy Reports 9 (2023) 230–238
www.elsevier.com/locate/egyr

2022 9th International Conference on Power and Energy Systems Engineering (CPESE 2022), Doshisha University, Kyoto, Japan, 9–11 September 2022

Hybridized high concentration photovoltaic unit with enhanced performance air gap membrane distillation unit via depositing reduced graphene oxide layer upon the condensation plate using electrophoretic deposition technique

Mohammed Rabie[a,b,c,*], M.F. Elkady[a,d], Tsuyoshi Yoshitake[c], A.H. El-Shazly[a,e]

[a] *Chemical and Petrochemicals Engineering Department, Egypt-Japan University of Science and Technology, Alexandria 21934, Egypt*
[b] *Mechanical Power Engineering Department, Mansoura University, El-Mansoura 35516, Egypt*
[c] *Department of Advanced Energy Science and Engineering, Kyushu University, Kasuga, Japan*
[d] *Fabrication Technology Department, Advanced Technology and New Materials Research Institute (ATNMRI), City of Scientific Research and Technological Applications, Alexandria, Egypt*
[e] *Chemical Engineering Department, Faculty of Engineering, Alexandria University, Alexandria 11432, Egypt*

Received 18 October 2022; accepted 22 October 2022
Available online xxxx

Abstract

Amongst the membrane distillation techniques, the air gap configurations showed an outstanding thermal efficiency, while a decline in productivity was recorded due to the additional thermal and mass resistances. The current study proposes minimizing the additional thermal and mass resistances by altering the condensation process to dropwise condensation. Depositing a layer of reduced graphene oxide using the electrophoretic deposition technique on the copper condensation plate was investigated to obtain a hydrophobic nature and attain dropwise condensation. Moreover, different operating conditions were examined for the optimum conditions, which were 45 V, 30 s, 1 cm, and 0.5 mg/ml, for the applied voltage, deposition time, distance between electrodes, and concentration, respectively. This modified condensation plate was investigated experimentally on the lab-scale test rig and showed an improvement in the productivity of 12.5% and 28.5% at the minimum and maximum feed temperatures, respectively. On the other hand, solar energy was utilized to eliminate the heating source required for the membrane distillation unit. A high concentration photovoltaic (HCPV) unit was introduced numerically in the current work with 36 multijunction cells. Furthermore, a microchannel heat sink was successfully designed to keep the cells from thermal degradation. The numerical results showed that the HCPV system could supply hot water up to 55 °C and produce electric power up to 230 W.

Peer-review under responsibility of the scientific committee of the 9th International Conference on Power and Energy Systems Engineering, CPESE, 2022.

Keywords: High concentrator photovoltaic; Membrane distillation; Reduced graphene oxide; Electrophoretic deposition

* Corresponding author at: Chemical and Petrochemicals Engineering Department, Egypt-Japan University of Science and Technology, Alexandria 21934, Egypt.
E-mail address: mohammedrabie@mans.edu.eg (M. Rabie).

https://doi.org/10.1016/j.egyr.2022.10.384

Peer-review under responsibility of the scientific committee of the 9th International Conference on Power and Energy Systems Engineering, CPESE, 2022.

1. Introduction

Membrane distillation (MD) attracts global attention due to its operation mechanism, which needs only a low temperature difference on the membrane surfaces [1,2]. Accordingly, this temperature difference initiates a difference in the vapor pressure on both sides of the membrane [3]. And simultaneously, this potential difference drives the vapor through the membrane's pores and condenses on the other side. There are four main configurations depending on the vapor condensation process, which are illustrated in detail in [4–7]. The current work introduces the air gap membrane distillation type (AGMD), which is schematically shown in Fig. 1. In this configuration, the vapor formed at the feed side is transferred through the membrane pores and condenses on the condensation surface of the cooling channel.

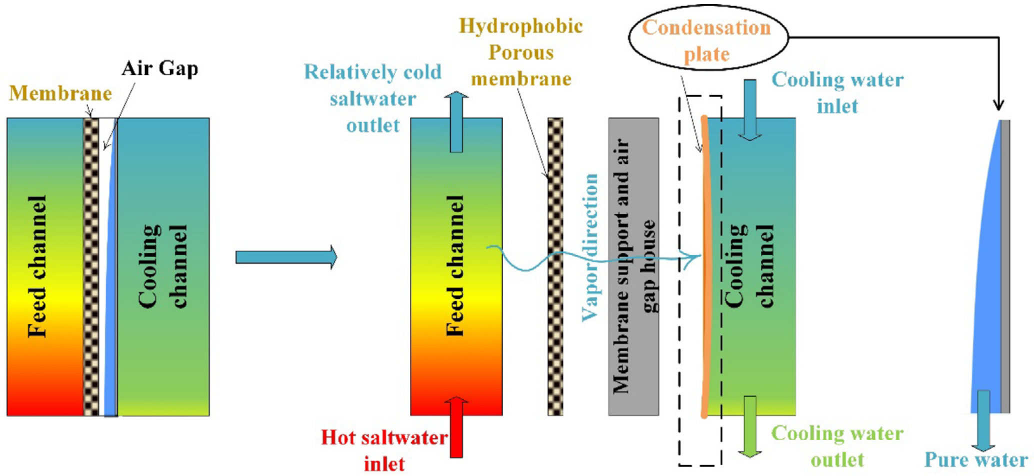

Fig. 1. Air gap membrane distillation unit.

Although AGMD proved the highest thermal efficiency among all other MD configurations, the low amount of produced freshwater is still a challenge [4]. Two novel AGMD designs have been introduced to recover the energy and be more economical [8]. The authors concluded that the proposed system thermal performance was significantly enhanced and recorded a 38.62% increase in productivity. Altering the condensation mechanism from film to dropwise is proved to dramatically improve the heat transfer process [9,10], besides mitigating the formed film's thermal resistance. In addition, finding renewable energy as a heating source is mandatory for MD to compete with other techniques.

No one can ignore the recent impressive advancement in solar energy applications and their availability. One of its new advancements was the multijunction cells (MJ), which considerably improved the electric efficiency to about 46%, instead of 10%–20% recorded for the conventional photovoltaic cells [11]. Furthermore, this type should be utilized with lenses or mirrors to concentrate the sunlight upon a considerably smaller MJ area, reducing the cost considerably [12]. The highlighted drawback of this type is overheating due to the high concentration of solar energy, which needs an adequate heat sink to eliminate any thermal failure [13]. A successful hybridization of HCPV/MD for water and electricity production was introduced in [14,15].

Accordingly, the originality of this study is to modify the condensation surface of the AGMD to add a hydrophobic nature and alter the condensation process to be dropwise. This was conducted by depositing a reduced graphene oxide layer upon the condensation surface via electrophoretic deposition. Moreover, hybridizing the AGMD with an HCVD unit eliminates the required heating source and simultaneous electric power production.

2. System components

The proposed hybrid system is illustrated as shown in Fig. 2, which comprises two main parts. The upstream part is the HCPV unit which contains 36 cells oriented as indicated in the figure, with a microchannel heat sink attached at its bottom to manage the thermal load. A Fresnel lens is mandatory in this type of photovoltaic to concentrate the solar energy upon the small multijunction cells, as illustrated in Fig. 2. The exit cooling fluid is

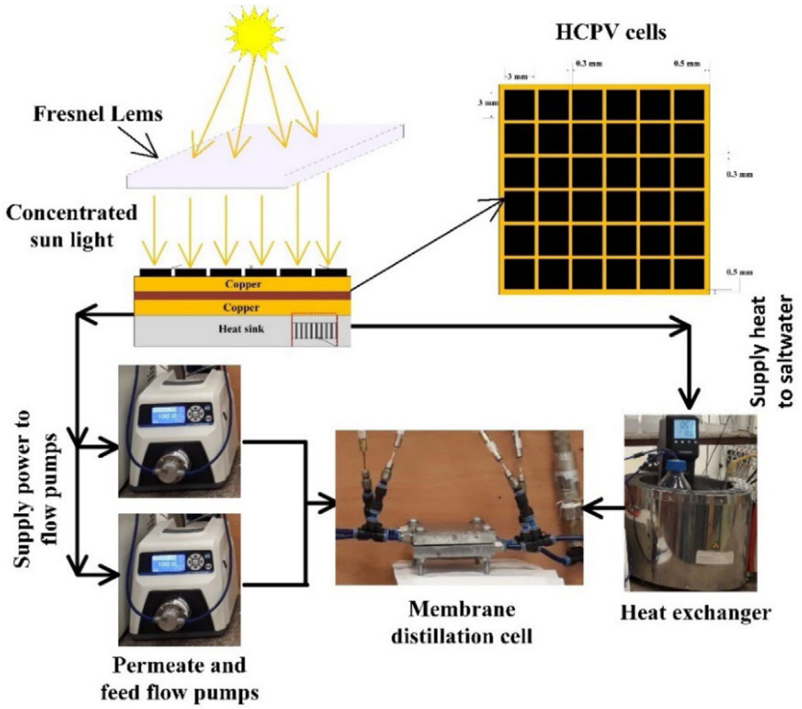

Fig. 2. Hybrid HCPV/MD system proposed for the current study.

optimized numerically for successfully managing the thermal load and to exit with adequate temperature for the AGMD unit. The heat exchanger shown in the figure is introduced to transfer the thermal energy from the cooling fluid to the saline water to be used as a feed to the AGMD unit. The second part is the downstream AGMD, which consists of two flow pumps and the membrane cell.

3. Numerical simulation

The HCPV unit was introduced numerically using Ansys 2020 software. The model was designed, discretized, tested for mesh dependence, and validated with previous work from the literature. The authors' published works introduced the mesh dependence step and validation [14,15]. Table 1 shows the validation results, and as could be seen the maximum error recorded was about 1%, which proved the validity of the presented numerical simulation model.

Table 1. Validation of the presented model with [12].

%Cell efficiency	Cell temperature [12]	Cell temperature (present)	%Error
0	54.5916	54	1.095556
30	45.1997	44.8052	0.880478
40	41.961	41.65	0.746699
50	38.659	38.4156	0.633597
60	35.2805	35.1429	0.391544

Moreover, suitable assumptions and boundary conditions have been set similar, as illustrated in [14,15]. The key parameters to control the whole performance of both HCPV and AGMD units are the coolant flow rate and the solar concentration ratio (CR), which is defined as how much solar irradiance is concentrated upon the multijunction cell. Increasing the CR increases the received solar heat flux, which needs more cooling. Accordingly, a numerical investigation is mandatory to study the overlapping effect of both parameters above.

3.1. Mathematical model

The governing equations for the presented HCPV model are the mass, momentum, and energy conservation equation which reduced due to the preset assumption to that presented in the authors' published work [14]. Furthermore, the produced electric power, cell conversion efficiency, and the excess thermal energy removed from the HCPV model (i.e., thermal energy removed by the heat sink and supplied as a heat generation for the numerical model) could be expressed as follows [15,16]:

$$P_{Electric} = \eta_{Cell}.I.CR.\alpha.A \tag{1}$$

$$\eta_{Cell} = \eta_{ref} - 0.00046\left(T_{cell} - 25\right) \tag{2}$$

$$q_G = \frac{\left(1 - \eta_{Cell}\right).I.CR.\alpha.A}{V} \tag{3}$$

I, CR, α, A, η_{Cell}, η_{ref}, and V are the solar irradiance (1000 W/m^2 for this study), concentration ratio, absorptivity, surface area, cell efficiency, reference efficiency at 25 °C, and the germanium volume, respectively.

4. Experimental work

4.1. Electrophoretic deposition

The reduced graphene oxide depositing process on the copper condensation plate was conducted via electrophoretic deposition. The cell used for deposition is homemade, as illustrated in Fig. 3. Graphene oxide (purchased from Sigma Aldrich), or could be prepared for economic purposes as presented in [17], is used to prepare the deposition solution according to the procedures shown in [18]. The substrate for deposition is copper (purchased from the local market) of dimensions 90 * 90 * 0.5 mm, of which 45 * 45 mm is the actual active area. Moreover, different operating conditions such as applied DC voltage, deposition time, the distance between the plates, and the concentration have been changed to get the optimum operating conditions.

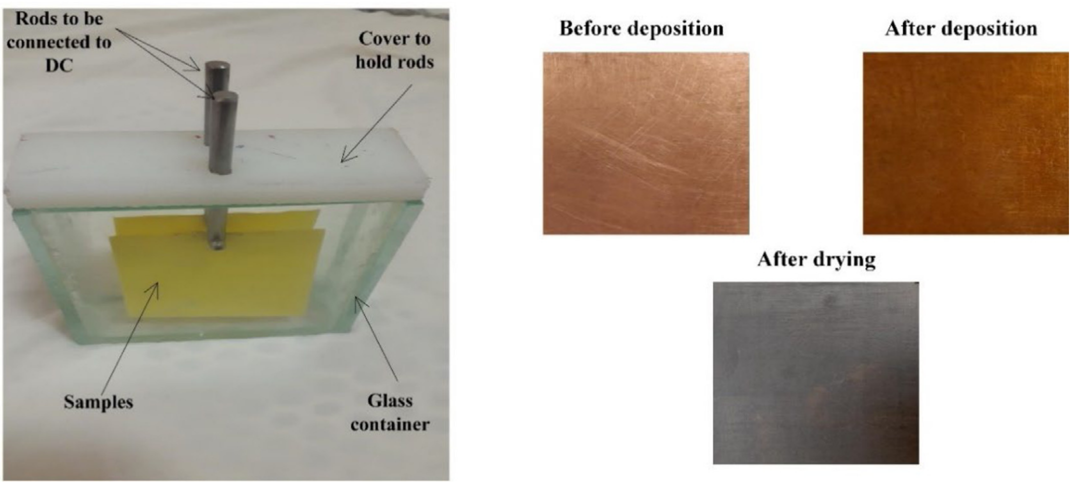

Fig. 3. Actual photographs of the depositing cell and the copper substrate at each step.

4.2. AGMD unit

AGMD system consists of the MD cell, flowing pumps, and the heat exchanger for feed water heating, as illustrated in Fig. 2. In addition, measuring instruments were mounted on the test rig to capture the different operating parameters such as flow rate (on the pump screen), thermocouples at both inlet ports, and pressure gauge.

5. Results and discussion

As illustrated before, the authors introduced a hybrid system with two major parts. The results of each part will be presented separately. First, the numerical simulation results of the HCPV unit and coolant flow rate optimization will be introduced, followed by the experimental results of electrophoretic deposition and AGMD performance.

5.1. The HCPV numerical simulation results

The cells' surface temperature is limited to 110 °C [16], so optimizing the coolant flow rate is very important to operate within the recommended limit. In addition, temperature uniformity also should be considered, which is defined as the deviation between the minimum and maximum temperatures, to prevent hot spots on the cells' surfaces [19–21]. The impacts of changing both coolant flow rate and concentration ratio on the cells' temperature and the temperature uniformity are presented separately in Figs. 4 and 5, respectively. There will be a tradeoff between the maximum temperature and the coolant outlet temperature, as seen in Fig. 4. For example, at the lowest flow rate, the maximum recorded cell temperature was about 110 °C, while the coolant outlet temperature was 55 °C, at a concentration ratio of 2000. Although the cell surface temperature was high, it is still in the recommended range, so it is suitable for AGMD feed.

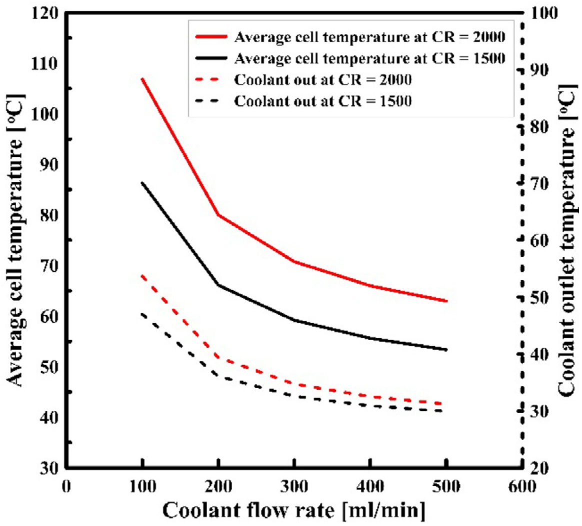

Fig. 4. Coolant flow rate impact on cells' temperature and available coolant outlet temperature.

Moreover, the influence of coolant flow rate on electric power and efficiency is presented in Fig. 6. As could be seen, increasing the flow rate improves both electric efficiency and power, which is attributed to the relation between the electric efficiency and the average cell temperature [16]. On the other hand, the effect of Re number on Nu has been introduced in Fig. 7. It shows that increasing Re positively affects the Nu and consequently the heat transfer process.

5.2. Experimental work results

The first step was to deposit a reduced GO layer upon the condensation plate to add the hydrophobicity nature to the condensation plate to alter the condensation mechanism from film to dropwise condensation. The operating conditions of the deposition process were changed to obtain the optimum operating conditions. The applied voltage and the deposition time studied ranges were 20–40 V and 15–45 s, respectively, whereas the distance between electrodes and the concentration were kept fixed at 1 cm and 0.5 mg/ml, respectively. Although all introduced conditions showed a hydrophobic surface (i.e., contact angle higher than 90°), the optimum conditions were found to be 45 V and 30 s for the applied voltage and deposition time, respectively, which gives a uniform deposited

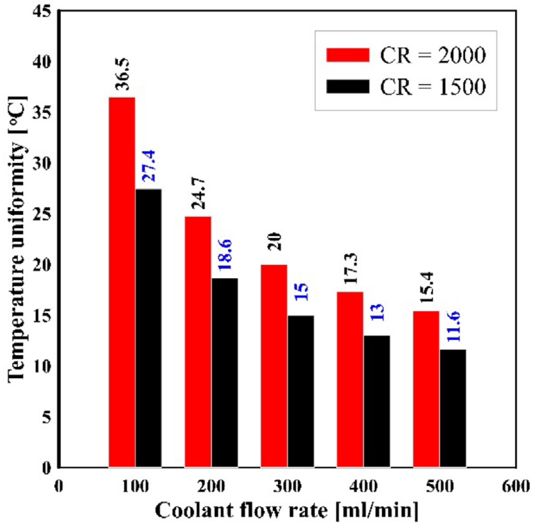

Fig. 5. Coolant flow rate impact on the cells' temperature uniformity.

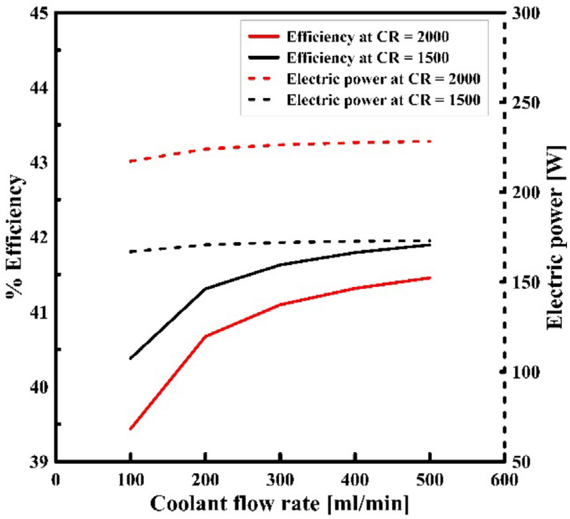

Fig. 6. Coolant flow rate impact on electric power and efficiency.

layer and, therefore, valid for the dropwise condensation. The deposited reduced GO on the condensation surface and actual photograph of the water on it are shown in Fig. 8.

Moreover, the condensation plate was then examined on the AGMD with and without the reduced GO layer to highlight the effect of altering the condensation mechanism from film to dropwise condensation. The operating conditions were fixed at 20 °C cooling water inlet temperature, 10,000 ppm feed water salinity, and 500 ml/min flow rate in feed and cooling channels, while the hot water temperature effect was changed from 50 to 80 °C to highlight its impact on the system productivity. Fig. 9 shows the effect of increasing the hot water temperature on the rate of pure water production (permeate flux) for the two cases of the condensation plate (with and without the deposited layer of reduced GO). As seen from the figure, depositing reduced GO on the condensation plate showed

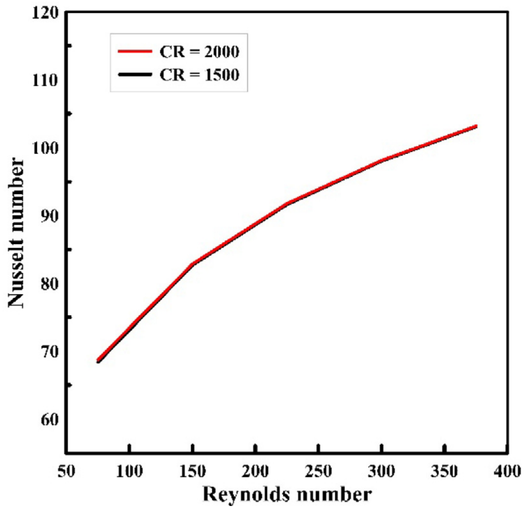

Fig. 7. Impact of flow Re on the average Nu.

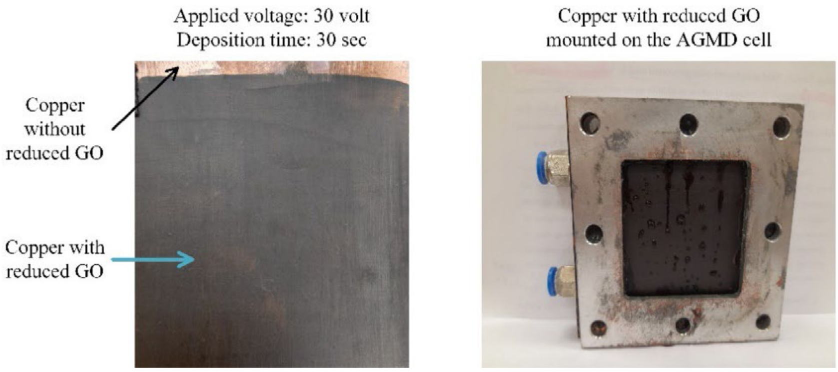

Fig. 8. Actual photos for the deposited reduced GO layer on the condensation plate.

higher productivity, which may be attributed to altering the condensation mechanism from film to dropwise. This may eliminate the additional thermal resistance formed by the condensed film on the condensation plate, therefore providing a higher temperature difference and consequently vapor pressure difference on the membrane surfaces, which is the main driving force that controls the system productivity.

6. Conclusion

The designed microchannel heat sink shows successful management for the thermal load of the HCPV unit and simultaneously provides hot water to be the heating source for the AGMD unit. The recommended coolant outlet temperature was 55 °C, at a concentration ratio and flow rate of 2000 and 100 ml/min, respectively. Moreover, the deposition of a reduced GO was experimentally introduced via electrophoretic technique on the condensation plate at 45 V and 30 s, applied voltage and deposition time, respectively. This layer shows a hydrophobic nature that was proved by the measured water contact angle. The impact of this deposited layer on the AGMD performance was investigated experimentally at different feed inlet temperature and showed a significant improvement. For instance, at the lowest studied feed inlet temperature, the productivity increased from 4 to 4.5 kg/m^2 h, and at the highest investigated temperature, it recorded a 28.5% enhancement. Overall, the proposed work showed a successful hybridization and a significant improvement in the AGMD productivity due to the modified condensation surface.

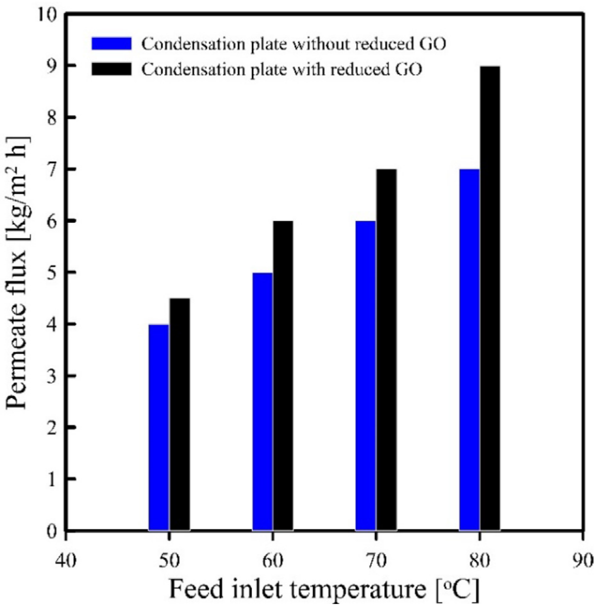

Fig. 9. Effect of feed inlet temperature on the productivity for the condensation plate with and without the reduced GO layer.

Declaration of competing interest

The authors declare that they have no known competing financial interests or personal relationships that could have appeared to influence the work reported in this paper.

Data availability

No data was used for the research described in the article.

Acknowledgments

We thank the Egypt-Japan University of Science and Technology (E-JUST) and the Ministry of Higher Education in Egypt for supporting us. In addition, the authors acknowledged the support from the Center for Japan-Egypt Cooperation in Science and Technology, Kyushu University. We also wish to show our appreciation to Dr. Asmaa Elrasheedy for her invaluable support.

References

[1] Ismail MS, Mohamed AM, Poggio D, Walker M, Pourkashanian M. Modelling mass transport within the membrane of direct contact membrane distillation modules used for desalination and wastewater treatment: Scrutinising assumptions. J Water Process Eng 2022;45:102460. http://dx.doi.org/10.1016/j.jwpe.2021.102460.

[2] Elrasheedy A, El Kady MF, Bassyouni M, Yoshitake T, El Shazly AH. Enhancement of Antiwetting properties of polystyrene nanofibrous membrane by doping with graphene nanoplatelets. Mater Sci Forum 2022;1060:83–8. http://dx.doi.org/10.4028/p-suy72p.

[3] Choi J, Cho H, Choi Y, Lee S. Combination of computational fluid dynamics and design of experiments to optimize modules for direct contact membrane distillation. Desalination 2022;524:115460. http://dx.doi.org/10.1016/j.desal.2021.115460.

[4] Alkhudhiri A, Darwish N, Hilal N. Membrane distillation: A comprehensive review. Desalination 2012;287:2–18. http://dx.doi.org/10.1016/j.desal.2011.08.027.

[5] Rabie M, Elkady MF, El-Shazly AH. Effect of channel height on the overall performance of direct contact membrane distillation. Appl Therm Eng 2021;117262. http://dx.doi.org/10.1016/j.applthermaleng.2021.117262.

[6] Elrasheedy A, Rabie M, El-Shazly AH, Bassyouni M, El-Moneim AA, El-Kady MF. Investigation of different membrane porosities on the permeate flux of direct contact membrane distillation. Key Eng Mater 2021;889:85–90. http://dx.doi.org/10.4028/www.scientific.net/KEM.889.85.

[7] Elrasheedy A, Rabie M, El-Shazly A, Bassyouni M, Abdel-Hamid SMS, Kady MFEl. Numerical investigation of fabricated MWCNTs/polystyrene nanofibrous membrane for DCMD. Polymers (Basel) 2021;13. http://dx.doi.org/10.3390/polym13010160.

[8] Elhenawy Y, Moustafa GH, Abdel-Hamid SMS, Bassyouni M, Elsakka MM. Experimental investigation of two novel arrangements of air gap membrane distillation module with heat recovery. Energy Rep 2022;8:8563–73. http://dx.doi.org/10.1016/j.egyr.2022.06.068.
[9] Warsinger DM, Swaminathan J, Morales LL, Lienhard VJH. Comprehensive condensation flow regimes in air gap membrane distillation: Visualization and energy efficiency. J Membr Sci 2018;555:517–28. http://dx.doi.org/10.1016/j.memsci.2018.03.053.
[10] Bahrami HRTalesh, Azizi A, Saffari H. Dropwise condensation heat transfer enhancement on surfaces micro/nano structured by a two-step electrodeposition process. J Cent South Univ 2019;26:1065–76. http://dx.doi.org/10.1007/s11771-019-4071-1.
[11] Ali AYM, Abo-Zahhad EM, Elkady MF, Ookawara S, El-Shazly AH, Radwan A. Temperature uniformity enhancement of densely packed high concentrator photovoltaic module using four quadrants microchannel heat sink. Sol Energy 2020;202:446–64. http://dx.doi.org/10.1016/j.solener.2020.03.106.
[12] Valera A, Fernández EF, Rodrigo PM, Almonacid F. Feasibility of flat-plate heat-sinks using microscale solar cells up to 10, 000 suns concentrations. Sol Energy 2019;181:361–71. http://dx.doi.org/10.1016/j.solener.2019.02.013.
[13] Aldossary A, Mahmoud S, AL-Dadah R. Technical feasibility study of passive and active cooling for concentrator PV in harsh environment. Appl Therm Eng 2016;100:490–500. http://dx.doi.org/10.1016/j.applthermaleng.2016.02.023.
[14] Rabie M, Ali AYM, Abo-Zahhad EM, Elqady HI, Elkady MF, Ookawara S, El-Shazly AH, Salem MS, Radwan A. Thermal analysis of a hybrid high concentrator photovoltaic/membrane distillation system for isolated coastal regions. Sol Energy 2021;215:220–39. http://dx.doi.org/10.1016/j.solener.2020.12.029.
[15] Rabie M, Elkady MF, El-Shazly AH. Hybrid membrane distillation/high concentrator photovoltaic system for freshwater production. Energy Rep 2022;8:112–9. http://dx.doi.org/10.1016/j.egyr.2021.11.067.
[16] Average T, Data E. Concentrator triple junction solar cell cell type: 3C44–3x3mm^2 application: Concentrating photovoltaic (CPV) modules. 2016.
[17] Madih K, El-Shazly AH, Elkady MF, Aziz AN, Youssef ME, Khalifa RE. A facile synthesis of cellulose acetate reinforced graphene oxide nanosheets as proton exchange membranes for fuel cell applications. J Saudi Chem Soc 2022;26:101435. http://dx.doi.org/10.1016/j.jscs.2022.101435.
[18] Hares E, El-Shazly AH, El-Kady MF, Hammad AS. Electrophoretic deposition of graphene oxide nanosheets on copper pipe for corrosion protection. Arab J Sci Eng 2019;44:5559–69. http://dx.doi.org/10.1007/s13369-019-03872-0.
[19] Elqady HI, Radwan A, Ali AYM, Rabie M, Abo-Zahhad EM, Ookawara S, Elkady MF, El-Shazly AH. Concentrator photovoltaic thermal management using a new design of double-layer microchannel heat sink. Sol Energy 2021;220:552–70. http://dx.doi.org/10.1016/j.solener.2021.02.003.
[20] Rabie M, Salem MS, Ali AYM, El-Shazly AH, Elkady MF, Ookawara S. Modeling of an integrated air gap membrane distillation unit utilizing a flat plate solar collector. Energy Rep 2020;6:1591–6. http://dx.doi.org/10.1016/j.egyr.2020.10.046.
[21] Ali AYM, Abo-Zahhad EM, Elqady HI, Rabie M, Elkady MF, El-Shazly AH. Impact of microchannel heat sink configuration on the performance of high concentrator photovoltaic solar module. Energy Rep 2020;6:260–5. http://dx.doi.org/10.1016/j.egyr.2020.11.248.